Interaction between the π-System of Toluene and the Imidazolium Ring of Ionic Liquids: A Combined NMR and Molecular Simulation Study

ARTICLE *in* THE JOURNAL OF PHYSICAL CHEMISTRY B · JANUARY 2009

Impact Factor: 3.3 · DOI: 10.1021/jp805573t · Source: PubMed

Interaction between the π-System of Toluene and the Imidazolium Ring of Ionic Liquids: A Combined NMR and Molecular Simulation Study

Thibaut Gutel,[†] Catherine C. Santini,*[,†] Agílio A. H. Pádua,*[,‡] Bernard Fenet,[§] Yves Chauvin,[†] José N. Canongia Lopes,[||] François Bayard,[†] Margarida F. Costa Gomes,[‡] and Alfonso S. Pensado[‡]

Université de Lyon, Institut de Chimie de Lyon, C2P2, Equipe Chimie Organométallique de Surface, UMR 5265 CNRS−ESCPE Lyon, 43 bd du 11 Novembre 1918, F-69626 Villeurbanne Cedex, France, Laboratoire de Thermodynamique des solutions et des Polymères, CNRS−Université Blaise Pascal, Clermont-Ferrand, France, Centre Commun de RMN, UCB Lyon 1−ESCPE Lyon, 43 bd du 11 Novembre 1918, F-69626 Villeurbanne Cedex, France, and Instituto de Tecnologia Química e Biológica, Oeiras, e Centro de Química Estrutural, Instituto Superior Técnico, Lisboa, Portugal

Received: June 24, 2008; Revised Manuscript Received: November 3, 2008

The solute−solvent interactions and the site−site distances between toluene and ionic liquids (ILs) 1-butyl-2,3-dimethylimidazolium bis(trifluoromethylsulfonyl)imide [BMMIm][NTf_2] and 1-butyl-3-methylimidazolium bis(trifluoromethylsulfonyl)imide [BMIm][NTf_2] at various molar ratios were determined by NMR experiments (1D NMR, rotating-frame Overhauser effect spectroscopy (ROESY)) and by molecular simulation using an atomistic force field. The difference in behavior of toluene in these ILs has been related to the presence of H-bonding between the C_2−H and the anion in [BMIm][NTf_2] generating a stronger association (>20 kJ·mol^{-1}) than in the case of [BMMIm][NTf_2]. Consequently, toluene cannot cleave this H-bond in [BMIm][NTf_2] which remains in large aggregates of ionic pairs. However, toluene penetrates the less strongly bonded network of [BMMIm][NTf_2] and interacts with [BMMIm] cations.

1. Introduction

Ionic liquids (ILs), also known as room temperature molten salts, are rapidly emerging as a new class of solvents for a variety of catalytic reactions. In many reports, differences in the rates and selectivities of the processes in ILs have been observed when compared to the corresponding reactions in molecular solvents. However, few details have been reported on the origin of these changes. In some catalytic reactions, the difference was related to the fact that ILs are a source of new ligands for the catalytic metal center, a catalyst activator, or even a cocatalyst or a catalyst itself. [1−3]

Other phenomena have been used to explain these differences in reactivity: the high viscosities and the highly ordered three-dimensional supermolecular polymeric networks of anions and cations linked by hydrogen bonds and/or Coulombic interactions.[4−9] Moreover, the segregation of these media in polar and nonpolar domains affects the solvation and the diffusion of ions and neutral molecules.[10] Yet, to our knowledge, no catalytic results have been related to the presence of π-interactions.

However, the unusually high solubility of aromatic compounds in ILs in comparison with aliphatic compounds has been explained by electrostatic interactions between the cations and the π-system of the aromatic compounds[11] and by the formation of liquid clathrates.[12] Also, a possible π···π interaction between alkylimidazolium or pyridinium cations and the aromatic π···π active moiety of the stationary phase could explain the selective separation of ILs by chromatography.[13] Finally, in chloroaluminate ionic liquids, the π-complexation between aromatic molecules and Lewis acid species ($Al_2Cl_7^-$) facilitates the extraction of aromatic hydrocarbons from aromatic/aliphatic mixtures.[14]

Nevertheless, the nature of the interactions between the π-system of the aromatic compounds and the charged ions of the ILs has been suggested but not experimentally demonstrated.

Yet, the significance and the importance of the interactions between aromatic rings and metallic ions (Li^+, Na^+, K^+, and Ag^+) or ammonium ions (NH_4^+, NMe_4^+) have been widely recognized.[15] This interaction, known as "π-cation interaction", plays an important role in both chemical and biological recognition and in organometallics.[16] The π-cation interaction with aromatics is arguably the strongest noncovalent force with a relatively high binding energy (from 10 to 30 kcal/mol). In addition, the conformation-controlling ability has opened up new methods for a stereoselective synthesis.[17] Besides the data provided by calculations, this π-cation interaction has been experimentally evidenced by mass spectrometry and NMR spectroscopy.[18−20]

The aim of this paper is to attempt to identify and experimentally confirm the nature of potential π-cation interactions between an unsaturated substrate and the imidazolium cation of ILs.

2. Results

2.1. Choice of the Experimental Conditions. The structures of imidazolium based ILs are governed by the cation nature and the strength of the hydrogen bond C_2−H−anion.[21,22] In the (1-butyl-2,3-dimethylimidazolium chloride) [BMMIm][Cl], the C_2 is substituted by an Me group, the cation−anion association energy is lower (<20 kJ·mol^{-1}) compared to (1-butyl-3-methylimidazolium chloride) [BMIm][Cl].[23] Moreover, the

* Corresponding authors. Fax: +33 472431795. Tel.: +33 472431794. E-mail: santini@cpe.fr (C.C.S.); agilio.padua@univ-bpclermont.fr (A.A.H.P.).
[†] Université de Lyon.
[‡] CNRS−Université Blaise Pascal.
[§] Centre Commun de RMN.
[||] Instituto Superior Técnico.

10.1021/jp805573t CCC: $40.75
Published on Web 12/10/2008

strength of this cation−anion association determines the availability of imidazolium cations to interact with the unsaturated substrates.[24,25] Consequently, these same cations $[BMMIm]^+$ and $[BMIm]^+$ were chosen.

In order to avoid competition with impurities such as chloride and water, bis(trifluoromethylsulfonyl)imide (NTf_2) based ILs were used because the corresponding ILs are hydrophobic, liquid at room temperature, and their purification is relatively well controlled.[26,27] Toluene (To) was also chosen because the methyl group provides a supplementary probe for NMR experiments. Finally, the microscopic structures of IL−toluene mixtures were investigated by molecular simulation, using an atomistic force field to describe the interactions and conformations experimentally studied.[28−30] This molecular model was parametrized specifically for ILs, in particular the electrostatic charge distributions and the torsion energy profiles, within the same philosophy as the widely used optimized potential for liquid simulations force field in its all-atom explicit version (OPLS-AA), by which toluene was also represented.[31] Thus, all ions and molecules are represented by fully flexible models in which an interaction site is attributed to each atom, composed of a Lennard-Jones site, to represent repulsive and dispersive forces, and of a partial charge. Here, partial charges were calculated ab initio at the MP2/cc-pVTZ(-f) level, on the most-stable confirmations of isolated ions.[28−30] The OPLS-AA force field is known to reproduce H-bonds accurately, and the electron density of aromatic systems is represented by the values of electrostatic charges on the relevant atoms combined with the Lennard-Jones sites that account for dispersion interactions. Explicit polarization of electron clouds by electric fields is not included in the present model. Although explicit polarization may be important to correctly reproduce dynamic properties of ionic liquids, structural features and thermodynamic quantities have been described to equivalent levels of accuracy using fixed-charge models. [32]

2.2. Solubility of Toluene. The solubility of toluene, evaluated by GC analyses, was equal to 38 ± 1 wt % in $[BMIm][NTf_2]$ and 36 ± 1 wt % in $[BMMIm][NTf_2]$ corresponding to 3 mol of toluene per mole of IL (molar ratio $R = 3$) These values are similar to those reported in the literature by means of ^1H (39 and 34 wt %, respectively), UV−visible spectroscopies (38 and 40 ± 2 wt %), and by gravimetric analyses.[12,33] The samples with molar ratio To/IL, R, varying from 0.1 to 3 were homogeneous monophasic solutions.

2.3. NMR Studies of Toluene/IL Systems. In order to investigate the interaction and the specific local structure of toluene with ILs, all systems were studied by ^1H ROESY experiments.

2.3.1. ^1H Chemical Shifts Evolution. The ^1H chemical shifts (δ) of toluene, neat, in $[BMMIm][NTf_2]$ and in $[BMIm][NTf_2]$, and those of the ILs, both neat and in the presence of toluene in molar ratios R ($R = 0$, 0.1, 0.5, 1, 2, and 3) are reported in Table 1. Scheme 1 describes the atom labeling of the cations $[BMMIm]^+$ and $[BMIm]^+$.

When R increased from 0 to 3, the proton chemical shifts of the imidazolium cycles were gradually shifted upfield, whereas all resonances of toluene were shifted downfield; Table 1.

2.3.2. ^1H Chemical Shift Evolution in Toluene: [BMIm][NTf$_2$]. For $R \leq 1$, there were no significant chemical shift variations (δ) for either the toluene or the imidazolium cycle $[BMIm]^+$, (**A** [CH_3 (ArMe)]; **B** [CH (Ar)]; **C** [NCH_3]; **D** [NCH_2] **E** [C_4H]; **F**[C_5H]; **G** [C_2H]); Table 1. The variation range, 0.01−0.02 ppm, is comparable with the uncertainty of the δ measurements. The variation of δC_2-H with toluene is

TABLE 1: ^1H Chemical Shift of the Toluene (in bold) in [BMIm][NTf$_2$] and [BMMIm][NTf$_2$] and of the Imidazolium Cycle (in italic) of [BMIm][NTf$_2$] and [BMMIm][NTf$_2$] as a function of the molar ratio To/ IL = R

	R		IL neat	to neat	0.1	$\Delta^a(\delta_0 - \delta_{01})$	0.5	$\Delta^a(\delta_0 - \delta_{0.5})$	1	$\Delta^a(\delta_0 - \delta_1)$	2	3	$\Delta^a(\delta_0 - \delta_3)$
[BMIm]	**CH_3(ArMe)**	**A**		**2.16**	**2.22**	**+0.06**	**2.22**	**+0.06**	**2.25**	**+0.07**	**2.19**	**2.22**	**+0.06**
	CH (Ar)	**B**		**7.08**	**7.1**	**+0.03**	**7.1**	**+0.03**	**7.1**	**+0.02**	**7.07**	**7.1**	**+0.03**
	NCH_3	**C**	*3.86*		*3.85*	*−0.01*	*3.82*	*−0.04*	*3.82*	*−0.04*	*3.77*	*3.52*	*−0.34*
	NCH_2	**D**	*4.13*		*4.12*	*−0.01*	*4.09*	*−0.04*	*4.06*	*−0.07*	*4.05*		*−0.08*
	C_4H	**E**	*7.36*		*7.34*	*−0.02*	*7.30*	*−0.04*	*7.25*	*−0.11*	*6.89*	*6.90*	*−0.46*
	C_5H	**F**	*7.44*		*7.41*	*−0.03*	*7.38*	*−0.06*	*7.33*	*−0.11*	*6.96*	*7.0*	*−0.44*
	C_2H	**G**	8.53		8.50	−0.03	8.46	−0.07	8.42	−0.11	8.4	8.12	−0.41
[BMMIm]	**CH_3(ArMe)**	**H**		**2.16**	**2.23**	**+0.07**	**2.28**	**+0.12**	**2.34**	**+0.18**	**2.46**	**2.52**	**+0.36**
	CH (Ar)	**I**		**7.08**	**7.10**	**+0.02**	**7.12**	**+0.04**	**7.19**	**+0.11**	**7.3**	**7.4**	**+0.32**
	NCH_3	**J**	*3.72*		*3.70*	*−0.02*	*3.64*	*−0.08*	*3.58*	*−0.14*	*3.58*	*3.60*	*−0.12*
	NCH_2	**K**	*4.03*		*4.01*	*−0.02*	*3.94*	*−0.1*	*3.89*	*−0.15*	*3.90*	*3.93*	*−0.1*
	C_4H	**L**	*7.23*		*7.21*	*−0.02*	*7.14*	*−0.09*	*7.08*	*−0.15*	*7.08*	*7.11*	*−0.12*
	C_5H	**M**	*7.30*		*7.28*	*−0.02*	*7.20*	*−0.1*	7.14		*7.12*	*7.14*	*−0.16*
	C_2-CH_3	**N**											

[a] $\Delta = \delta_0 - \delta_R$; δ_0 = the proton chemical shift of neat toluene or of the imidazolium ring; δ_R = the proton chemical shift of toluene and of the imidazolium ring for a molar ratio R.

SCHEME 1: Atom Labeling of the Cations [BMMIm]$^+$ and [BMIm]$^+$

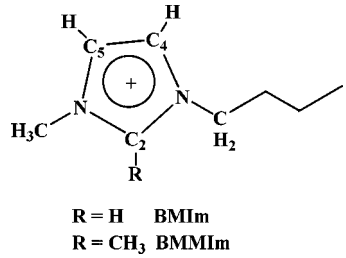

relatively smaller ($\delta_0 - \delta_1 = 0.1$ ppm when R varied from 0.1 to 3) than that with acetone-d_6, ($\Delta\delta = 0.4$ ppm when R varied from 0.05 to 0.95).[34] For $R \leq 1$, the interactions between toluene and [BMIm]$^+$ were probably very weak.

For $R \geq 1$, there was still no significant variation of δ(**A** [CH_3 (ArMe)]; **B** [CH (Ar)]) of the toluene. On the contrary, δ [BMIm]$^+$, (**E** [C_4H]; **F**[C_5H]; **G** [C_2H]), shifted upfield ($\delta_0 - \delta \geq 0.4$ ppm); Table 1. As reported in the NMR study on the interactions of imidazolium ionic liquids with acetone, the pronounced effect on the chemical shift of the imidazolium proton at high concentration could be related to a decrease in the strength of the C_2−H···NTf_2 hydrogen bonds. However, the aromatic molecules are in competition with NTf_2, which should be stronger hydrogen bond acceptors.[23] Consequently, the variation could be correlated to an alteration of the IL structure, in particular, the cation−cation interactions/distances, although a strong ionic ordering was still observed.[35−38]

2.3.3. ^{1}H Chemical Shift Evolution in Toluene: [BMMIm][NTf$_2$]. In toluene:[BMMIm][NTf_2] samples, when R varied from 0 to 3, a monotonously downfield shift for δTo (**H** [CH_3 (ArMe)]; **I** [CH (Ar)] and an upfield shift for δ [BMMIm] (**J** [NCH_3]; **K** [NCH_2]; **L** [C_4H]; M[C_5H]; **N** [C_2−CH_3]) was observed; Table 1. The variation of δ could be due to several contributing factors, such as, (a) the aromatic ring current effect (i.e., $\pi-\pi$ interaction), (b) C−H−π interaction between the cation and the toluene, (c) the anion effect, (d) the dilution effect, and (e) the electrostatic field effect.[39]

The aromatic ring current effect is well documented.[40] The chemical shifts of protons situated above or below the shielding cone of the aromatic ring are shifted upfield (i.e., shielding effect), whereas δ of protons located outside the shielding cone are shifted downfield. In our system, both the toluene and the [BMMIm] cation are aromatic. The aromatic ring current effect in neat toluene is stronger than that in neat [BMMIm][NTf_2] because toluene molecules are more tightly packed.[37] In our ILs, the cations are separated by the bulky NTf_2 anions preventing them from coming closer together, thus greatly reducing the aromatic current effect.[41] Therefore, δ(**I** [CH (Ar)]) of neat toluene was more upfield than δ(**L** [C_4H]; **M**[C_5H]) of neat [BMMIm][NTf_2].[39] The experimental results were consistent with the presence of the [BMMIm] cation in the shielding cone of the toluene ring current and of the toluene near the deshielding zone of the [BMMIm] ring current.

The C−H−π interaction between the [BMMIm] cation and proton **I** [CH (Ar)] as well as the interaction between the NTf_2 anion and proton **I** [CH (Ar)] could also induce a variation in the chemical shift for the protons. Indeed protons (**L** [C_4H]; **M**[C_5H]) form stronger hydrogen bonds with anions than with aromatics.[23] In this study, such factors could be considered as minor.

The NMR spectra carried out at various molar ratios of toluene in pentane and in 1,2-dimethylimidazole showed that the dilution effect did not lead to a noticeable variation of the ^{1}H chemical shift when $R \leq 1$.

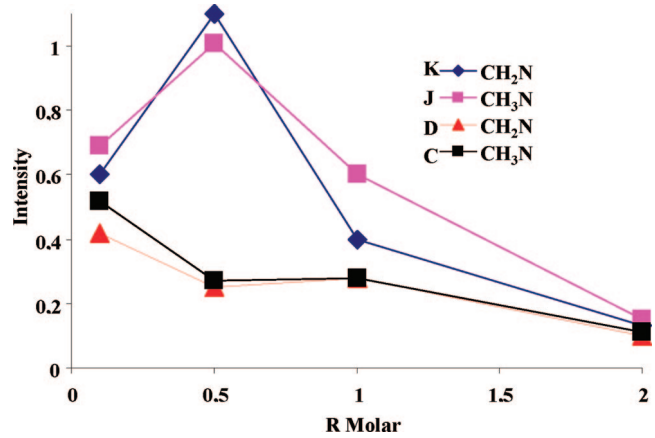

Figure 1. Variation of the intensity of integrals from ROESY experiments at various molar ratios (R) for (**J** [NCH_3]; **K** [NCH_2]) in To/[BMMIm][NTf_2] and for ([**C** [NCH_3]; **D** [NCH_2]) in To/[BMIm][NTf_2].

Finally, the electrostatic field effect was important when electrons surrounding the resonating nucleus are displaced by chemically bonded polar atoms such as fluorine. However, as no effect was observed in other media such as (pentane, cyclohexadiene) in the presence of [BMMIm][NTf_2], we could assume it to be negligible.

With the consideration of all these possible factors and the observed NMR results, the aromatic ring current effect seemed the dominant factor influencing the trend of chemical shift changes in the [BMMIm]$^+$ cation and the toluene. Indeed, the electronic density of the π-system of toluene decreased due to the interaction with the electron-deficient π-system of positively charged imidazolium rings, and vice versa. In our results, when $R \leq 1$, a ring current effect was detected in To/[BMMIm][NTf_2] but not in To/[BMIm][NTf_2].

2.3.4. ROESY Experiments. NOESY experiments exhibited very weak or null cross peak intensities. This was probably due to the fact that the quantity $\omega\tau c$ was such that the NOE intensity was close to the null point. Rotating frame NOE experiments (ROESY) allowed us to obtain positive NOEs irrespective of the long rotational correlation time due to the high viscosity of the system. In^{1}H−^{1}H ROESY techniques based on space cross relaxations, the selective irradiation of a proton group affects the intensities of integrals of all proton groups which were spatially close but not necessarily connected by chemical bonds. The method was based on the assumption of short-range intermolecular distances (4−5 Å).[42]

NMR ROESY experiments of To/[BMIm][NTf_2] and To/[BMMIm][NTf_2] samples with R varying from 0.1 to 3 were undertaken. The irradiation of δTo (**H** [CH_3 (ArMe)]) induced a negative resonance for each δ[BMMIm] (**J** [NCH_3]; **K** [NCH_2]; **L** [C_4H]; **M**[C_5H]; **N** [C_2−CH_3]) with an intensity proportional to the intensity of the intermolecular interaction, vide supra. The variation of the intensities of the negative resonance integrals for δ[BMMIm] (**J** [NCH_3]; **K** [NCH_2] is represented in Figure 1 (see also the Supporting Information).

For To/[BMMIm][NTf_2] mixtures, the ROESY intensity increased when R varied from 0 to 0.5 and then sharply decreased to zero when R varied from 1 to 2. On the contrary, for To/[BMIm][NTf_2] mixtures, no particular interaction was evidenced. The ROESY intensity was low when R varied from 0 to 1 and decreased to zero for $R > 1$.

The strength of the ROE signal is proportional to the inverse sixth power of the distance between the atoms, $I \propto 1/r^6$. In the liquid state, this relation is possible if the intermolecular association is tight enough to turn the intermolecular relaxation into "intramolecular" within the ion pair or ion−molecule association.[42] Highly structured, bulk ionic liquids seemed to fulfill these requirements, thus allowing the use of the intermolecular ROESY to derive lower limits for interionic distances.[4−9] Consequently, for $R \leq 1$, the intensity of the integrals (I_{To-IL}) could be considered as roughly inversely proportional to the intermolecular distances. Conversely, for $R > 1$ as the translational diffusion might play a dominant role with respect to the rotational tumbling of a putative tight toluene/[BMIm] or toluene/[BMMIm] association, the results of the ROESY experiments were not accurate.[42] For $R \leq 1$, the distance (r_{To-IL}) separating the irradiated Me(Ar) of the toluene and the protons of the groups N−CH_3 and N−CH_2 of the imidazolium cycle was defined by $r_{To-IL} = r_{ref}(I_{ref}/I_{To-IL})^{1/6}$.[43] The intensity of the reference integral (I_{ref}) was measured in the same experimental conditions. The reference distance (r_{ref}) is the distance between the protons **J** [NCH_3] and **L** [C_4H] (i.e., the geometric center of mass of all three protons) of the imidazolium rings determined from crystallographic data[21] and minimized using the molecular mechanics Tripos force field.[44,45] It was found to be equal to 2.98 Å.

For a molar ratio $R \leq 1$, the results indicated that the toluene was closer to the [BMMIm] cation than to the [BMIm] cation. The distances between **H** [CH_3(ArMe)] of toluene and both proton groups **J** [NCH_3]; **K** [NCH_2] of the [BMMIm] cation were almost identical. The toluene was found with a high probability in a plane parallel to the imidazolium ring. The extrapolation of the ROESY integrals showed that the toluene was located at c.a. 3 ± 0.5 Å from the imidazolium rings, a value in the range of reported distances between toluene−ammonium and benzene−[MMIm][PF_6] (3.0 and 3.5 Å, respectively).[36,46]

2.4. Structural Analysis from Molecular Dynamics Simulation. Alkylimidazolium ILs have been shown to self-organize in nanometer scale domains, with regions of high charge density composed of the cationic headgroups and the anions and regions of low charge density in which the alkyl side chains of the cations aggregate.[10,47] The polar regions constitute a 3D network, which is continuous due to of the high cohesive energy of the charged anions and head groups of the cations. The nonpolar regions constitute domains which, for relatively short side chains such as butyl, are largely noncontiguous, i.e., form small nonpolar pockets embedded in the continuous polar network.

In mixtures of such ILs with aliphatic hydrocarbons, the hydrocarbon molecules are solvated only in the nonpolar domains and do not interact with the charged network.[48] The situation was expected to be different for aromatic hydrocarbons, which interact with both the cation and the anion moieties of the charged domains.[49]

In Figure 2 are plotted site−site radial distribution functions between atoms in toluene and atoms in the [BMIm] cation, showing a strong association between the H atoms of the methyl group of toluene and the terminal C atom of the butyl side chain and relatively weak interactions with atoms of the imidazolium ring. Therefore, in [BMIm][NTf_2], the methyl group of toluene is solvated in the nonpolar domains, a situation similar to that obtained for saturated hydrocarbons. In contrast, the aromatic ring of toluene (represented by the aromatic H in Figure 2) is found with a similar probability in the vicinity of the aromatic ring and the side chain.

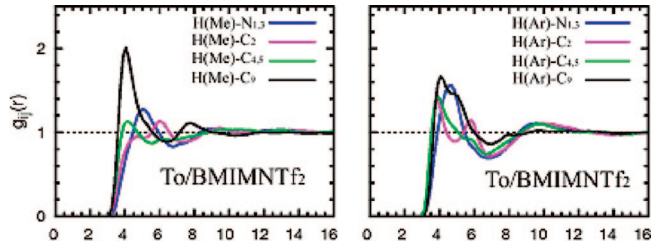

Figure 2. Radial distribution functions between protons in toluene, H(Me) of the methyl group and H(Ar) of the aromatic ring, and selected sites in the [BMIm] cation, including C9, the terminal carbon atom in the butyl side chain, for $R = 1$.

In Figure 3 is shown a comparison of radial distribution functions in To/[BMIm][NTf_2] and To/[BMMIm][NTf_2]. The most prominent feature is that both Me(Ar) and H(Ar) of toluene were found with a high probability closer to the carbon in position 2 of the imidazolium ring C_2−Me in [BMMIm][NTf_2], whereas no significant correlation existed in [BMIm][NTf_2]. The probability of finding the toluene methyl group in the vicinity of the terminal carbon of the butyl side chain was only slightly reduced in [BMMIm][NTf_2] when compared to [BMIm][NTf_2].[10] These results were consistent with the NMR experiments.

Detailed structural features are much better perceived in 3-dimensional spatial distribution functions, as shown in Figure 4. In [BMIm][NTf_2], there was found to be a high probability of finding the oxygen atoms of NTf_2 near to the C_2−H of the cation, and no significant presence of toluene methyl groups was seen in this region. The situation was completely different in [BMMIm][NTf_2], with a strong presence of toluene near the C_2−Me of the imidazolium. With both cations, toluene was also found above and below the imidazolium plane, at distances longer than those of closest cation−anion pairs.

Interactions of [BMMIm] with the anions were mainly through the C_4−H and C_5−H hydrogen atoms and also through the nitrogen atoms. These sites of the cation were then responsible for the cohesion of the charged network in the ionic liquid. In [BMIm], C_2−H participated very actively in cation−anion interactions, but as pointed out above, the C_2−Me site in [BMMIm] was preferentially associated with toluene.

The distribution of ions around a toluene molecule is also shown in Figure 5, for [BMIm][NTf_2]. The arrangement of ions was such that cation headgroups (the blue regions) are located above and below the aromatic ring, interacting with the π-system, whereas the oxygen atoms of the anions (the red regions) are located around the toluene molecule in the plane of the ring, interacting with the H(Ar).

This arrangement is typical of the solvation of aromatic molecules by ILs[36] and can also be observed in crystal structures.[49] The terminal Me of the alkyl chain of the imidazolium cation was found with a higher probability in regions of space between those occupied by cations and anions and particularly near the methyl group of toluene.

Since all experimental factors were the same (concentration, temperature, and identical conditions during the NMR experiments), the differences in the observed phenomena resulted from the nature of the ILs. As the NTf_2 anion was unchanged, the differences in these experiments were therefore mainly due to the nature of the cation. The alkylation at position C_2 of the imidazolium ring reduces the H-bond ability of the cation; for instance, Kamlet−Taft α values of [EMIm][BF_4] and [EMMIm][BF_4] are 0.73 and 0.40, respectively, and the same difference is reported between [BMIm][$N(CN)_2$] and [BMMIm][$N(CN)_2$], 0.533 and 0.373, respectively. Contrarily, the

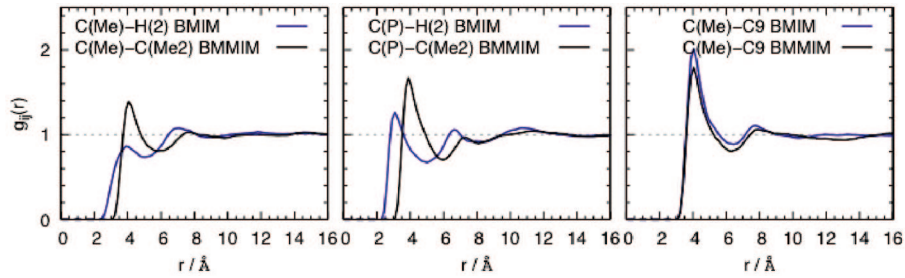

Figure 3. Comparison of site−site radial distribution functions between chosen atoms in toluene and in the cations, in To/[BMIm][NTf_2] and To/[BMMIm][NTf_2]. C(Me2) is the methyl group carbon in position C(2) of the imidazolium ring, and C9 is the terminal C atom from the alkyl side chain. C(P) is the para carbon in toluene, representing the location of the aromatic ring.

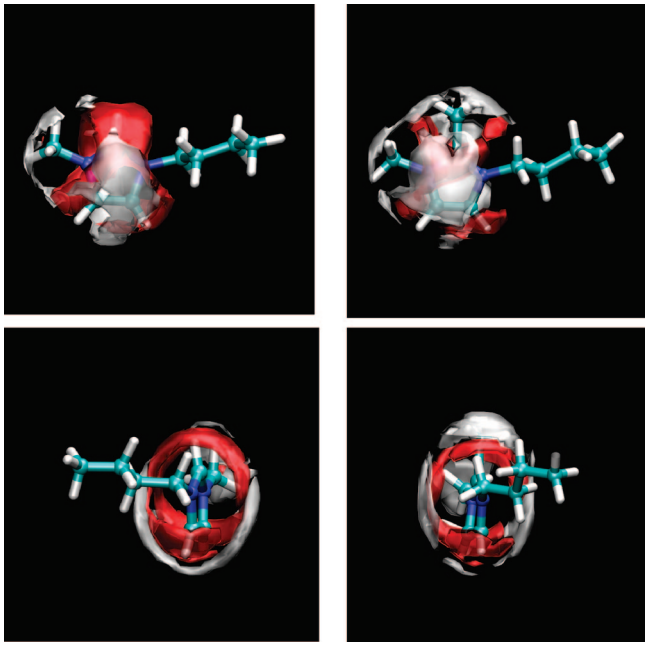

Figure 4. Spatial distribution functions around the C(2) carbon of the cations in To/[BMIm][NTf_2] (left) and To/[BMMIm][NTf_2] (right). Above and below are different views of the same isosurfaces. In red is plotted the isosurface corresponding to a local density of 4 times the average density of oxygen atoms from the NTf_2 anion. In white is plotted the isosurface corresponding to a local density of 2 times the average density of methyl carbons from toluene.

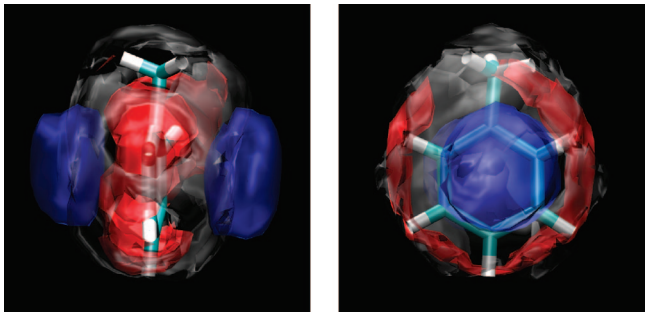

Figure 5. Spatial distribution functions around the toluene ipso C in To/[BMIm][NTf_2]. In blue is plotted the isosurface corresponding to a local density of twice the average density in C(2) carbon of the imidazolium cations. In red is plotted the isosurface corresponding to a local density of twice the average density of oxygen atoms from the NTf2 anion. In gray is plotted the isosurface corresponding to a local density of twice the average density of terminal methyl carbons from the butyl side chain C(9).

α value is similar whatever the nature of the alkyl chain ([BMIm][$N(CN)_2$] 0.533, [iBMIm][$N(CN)_2$] 0.544) influencing drastically its 3D organization and its ability to H-bond with the coexisting components. Indeed it has been shown that the cation−anion association energies are slightly lower (<20 kJ·mol^{-1}) for the ion pairs of [BMMIm][Cl] compared to those of [BMIm][Cl]. Moreover, the cations and anions of [BMMIm][Cl] are in general more ionic that those of [BMIm][Cl], and the positive charges in [BMIm][Cl] are localized on the peripheral H atoms and spread out over the C_2−H moiety, while in [BMMIm][Cl], the charge spread out over the C_2−H moiety resides entirely on C_2. Such localization of charge facilitates stronger Coulombic interactions.[23,50,51] Besides this effect related to interionic interactions, methylation of the C_2 position increased the affinity of the cation headgroup to nonpolar or weakly polar molecules that would not interact significantly with this site in the case of the hydrogenated counterpart.

At molar ratios R less than 1, in the 1,3-dialkylimidazolium cation [BMIm], the H(2) acidic proton was strongly linked to the anion by hydrogen-bonding, and consequently, the imidazolium headgroup of the cation [BMIm] could not interact easily with π-systems because aromatic molecules could not cleave this hydrogen-bond. This assessment was supported by two recent results. On one hand, the IR and Raman spectra of the dilute solution of [EMIm][BF_4] in CH_2Cl_2 prove that ion pairing is not destroyed by the solvent.[52] On the other hand, solid−liquid phase diagram study and X-ray structure determination show experimentally that the aromatic plane of benzene and some of the [EMIm] cations are stacked in parallel arrangements (the crystals showing two orientations quasi perpendicular to each other).[49] Also in the case of Holbrey's crystals, the [MMIm] cations occupy positions above and below the plane of the benzene aromatic ring.[12]

The present NMR and simulation results have indicated that at high toluene concentrations, for both ILs, the structure of the To/IL mixtures are similar. Near the solubility limit, the high concentration of toluene brought the highly charged network of the ionic liquid close to disruption, but solvation of the IL by toluene was not strong enough to impede phase separation, with formation of a toluene phase. However, there were important differences between the two ionic liquids in the intermediate concentration range. With [BMIm] there were three H-bond sites in the imidazolium ring interacting with the anions, C_2−H, C_4−H, and C_5−H, and toluene could disrupt but a few of these interionic H-bonds. With [BMMIm], there were only two such H-bonds, and toluene found a preferential site near the methyl group in C_2−Me. Moreover, for [BMMIm][NTf_2], the present NMR and modeling results indicated that toluene was coplanar to the imidazolium ring and presented a very strong interaction for molar ratio $R = 0.5$ or 1. Consequently, toluene had probably penetrated the IL network and was located between two imidazolium ring planes with which it strongly interacted. The solute may be viewed as intercalating in the charge distribution of the

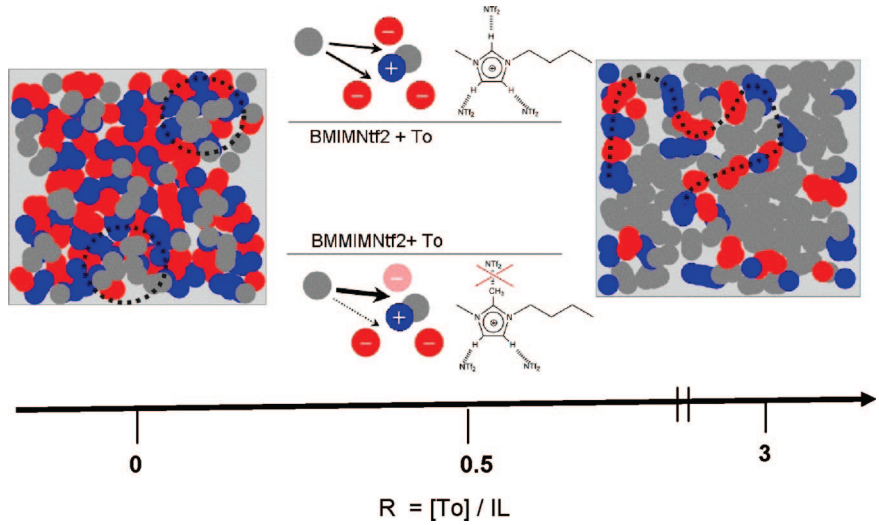

Figure 6. Schematic representation of the structure of To/IL mixtures. The charged headgroups of the cations are in blue and the alkyl side chains in gray, anions are colored red, and toluene is also in gray. The simulation snapshot on the left is a cut obtained from a simulation box of pure IL, where association of the nonpolar side chains can be seen. The snapshot on the right corresponds to a concentration of toluene close to saturation ($R = 3$) where it is observed that the positively and negatively charged parts remain in continuity, although the nonpolar regions occupy the majority of the volume. Between the two snapshots are represented the differences in the interaction of toluene with the two cations. Although the preferred interaction is in both cases with the nonpolar side-chain, it is in [BMMIm][NTf_2] that toluene can intercalate between the cation and the anion in a more localized manner.

TABLE 2: Densities and Viscosities, at 298.15 K and Atmospheric Pressure, of Mixtures of [BMMIm][NTf_2] and Toluene

x_{IL}	n_{tol}/n_{IL}	ρ/g·cm^{-3}	η/mPa·s
0.9068	0.103	1.4016	80.16
0.5002	0.999	1.2856	18.61
0.3317	2.015	1.2041	7.758
0.2862	2.494	1.1786	6.037
0.2500	3.000	two phases	

neat liquid.[53] The differences in the solvation of toluene by the ionic liquid are represented in a schematic way in Figure 6.

3. Conclusion

The role of π-cation interactions, crucial in biochemistry, is reported in most cases for the interaction of ammonium cations with aromatic rings. Although ILs are only composed of charged species, the presence and the influence of π-interaction has never been detailed. In order to favor π-interactions between aromatic substrates and cations of ILs, two aromatic and planar cations—[BMIm] and [BMMIm]—were chosen and associated to the NTf_2 anion to generate hydrophobic ILs, liquid at room temperature.

The results of the NMR studies (chemical shift evolution, ROESY experiments) and of the molecular simulations confirmed that toluene was closer to the methyl group at the end of the butyl chain of [BMIm][NTf_2] while it was closer to carbon C_2—Me of the imidazolium ring of [BMMIm][NTf_2] and in a parallel plan to [BMMIm] cation.

This difference was related to the presence of H-bonding between the C_2—H and the anion in [BMIm][NTf_2] generating a stronger association (>20 kJ·mol^{-1}) than in the case of [BMMIm][NTf_2]. Toluene did not cleave the H-bond in [BMIm][NTf_2], which remained aggregates in large groups of ionic pairs. In contrast, toluene penetrated the less strongly bonded network of [BMMIm][NTf_2] and interacted with [BMMIm] cations.

4. Experimental Section

1-Methylimidazole (>99%) and 1,2-dimethylimidazole (>98%) (Aldrich) were distilled prior to use. Anhydrous toluene (99.8%) (Aldrich) was distilled aver NaK alloy and stored on zeolites. Bis(trifluoromethanesuflonyl)imide lithium salt (>99%, Solvionic company) was used without further purification

Ionic liquids, synthesized as previously reported,[26] were dried overnight under high vacuum and stored in a glovebox (Jacomex) in order to guarantee rigorously anhydrous products.

4.1. Determination of Solubility of Compounds in Ionic Liquid. In a glovebox, 2 mL of toluene was added to 1 mL of each of the ionic liquids. The resulting systems were stirred over 24 h at 30 °C leading to a biphasic system. A 0.1 mL portion of the lower phase (IL rich phase) was dissolved in 0.9 mL of acetonitrile in the presence of an internal standard (toluene or benzene).

4.1.1. GC Analyses. The products were quantitatively analyzed by gas chromatography on a HP6890 chromatograph equipped with a flame ionization detector (FID) and an Al_2O_3/KCl column ($L = 50$ m, $\phi_{int} = 0.32$ mm, film thickness $= 5$ μm). The injector and detector temperature was 230 °C, and the injection volume was 1 μL. The temperature was fixed at 190 °C.

4.2. Determination of the Viscosity of Samples Toluene—[BMMIm][NTf_2]. The mixtures of different toluene composition where prepared gravimetrically. The ionic liquid was first introduced in a glass vial, and then, the appropriate amount of toluene was added and the glass vial was sealed. The vial was completely field with the liquid mixture in order to minimize the volume of the vapor phase in equilibrium with the liquid solution and to reduce the error in composition due to differential evaporation. The uncertainty of the mole fraction is estimated as ±0.0001. The viscosity of the mixtures was measured at 298.15 K (controlled to within 0.01 K and measured with an accuracy better that 0.05 K) using a rolling ball viscometer from Anton Paar, model AMVn, equipped with capillary tubes of 3 and 1.6 mm in diameter. Before starting the measurements, we have calibrated the 3 mm diameter tube as a function of temperature and angle of measurement, with standard viscosity

oil from Cannon (N35). The 1.6 mm diameter tube was calibrated with water by the manufacturer. The overall uncertainty on the viscosity is estimated as ±1.5%.

The densities of the mixtures, necessary to calculate the viscosities were measured in an Anton Paar vibrating tube densimeter model 512 P, at the same temperature (measured by a calibrated PRT with an accuracy of 0.02 K). The densimeter was calibrated using tridistilled water, toluene, and a sodium chloride aqueous solution (1 M in concentration).

4.3. NMR Studies. Approximately 0.3 mL samples with molar ratios R varying from 0.1 to 3 were introduced into a 5 mm NMR tube. A stem coaxial capillary tube loaded with CD_2Cl_2 was inserted into the 5 mm NMR tube to avoid any contact between the deuterated solvent and the analyzed mixture. The deuterium in CD_2Cl_2 was used for the external lock of the NMR magnetic field and the residual $CHDCl_2$ in CD_2Cl_2 was used as the ^1H external reference at 5.32 ppm. When ^1H data are obtained in this way, the reference signal of $CHDCl_2$ will remain as a constant and not be affected by changes in sample concentration.

4.3.1. NMR Instrumentation. ^1H 1D and ROESY experiments were carried out on a Bruker DRX 500 instrument at 298 K (nominal) with a resonance frequency at 500 130 MHz.

4.3.2. ROESY (Rotational Nuclear Overhauser Effect Spectroscopy). The 2D sequence was built with the scheme proposed by Bodenhausen.[54] The mixing time (200 ms) is split into 2 parts separated by a π-pulse. At each side of the spin lock, the B1 field is ramped linearly (4.5 ms) to ensure adiabatic conditions for spinlock. During the first spinlock pulse, the frequency is shifted to O1 + Δf whereas the second pulse frequency is set to O1 − Δf, where O1 is the offset frequency and Δf is set to give a B1 field at the magic angle. By this way, the ROESY response is roughly constant across the spectra of interest.

For a 1D sequence, PFGSE (pulse field gradient spin echo for selective excitation) have been used and spinlock followed the same scheme as previously.

4.4. Computer Simulation Details. Molecular dynamics simulations were performed of condensed-phase To/BMIMNTf$_2$ and To/[BMMIm][NTf$_2$] mixtures using the DL_POLY program.[55] System sizes were chosen so as to contain about 10 000 atoms, and so, the numbers of cations, anions, and toluene molecules varied according to composition (64 toluene and 192 ion pairs for $R = {}^1/_3$, 160 toluene and 160 ion pairs for $R = 1$, and 300 toluene and 100 ion pairs for $R = 3$). Initial low-density configurations, with ions and molecules placed at random in period cubic boxes, were equilibrated to attain liquid like densities and structures at 300 K and 1 bar. Temperature and pressure were maintained using Nosé-Hoover thermostat and barostat. Production runs then took 600 ps with an explicit cutoff distance of 16 Å for nonbonded interactions, and long-range corrections applied for repulsive−dispersive interactions. Electrostatic energies were calculated using the Ewald summation method with a relative accuracy of 10^{-4}. Structural quantities such as radial and spatial distribution functions were calculated from configurations generated during the production runs.

Supporting Information Available: Intensity vs R data. This material is available free of charge via the Internet at http://pubs.acs.org.

References and Notes

(1) Wasserscheid, P. *In Ionic Liquids in Synthesis*; Wiley-VCH: Weinheim, 2003; pp 213−257.
(2) Olivier-Bourbigou, H.; Vallee, C. *In Multiphase Homogeneous Catalysis*; Wiley-VCH: Weinheim, 2005; Vol. 2, pp 413−431.
(3) Hintermair, U.; Gutel, T.; Slawin, A. M. Z.; Cole-Hamilton, D. J.; Santini, C. C.; Chauvin, Y. *J. Organomet. Chem.* **2008**, *693*, 2407–2414.
(4) Bonhote, P.; Dias, A.-P.; Papageorgiou, N.; Kalyanasundaram, K.; Graetzel, M. *Inorg. Chem.* **1996**, *35*, 1168–78.
(5) Mele, A.; Romano, G.; Giannone, M.; Ragg, E.; Fronza, G.; Raos, G.; Marcon, V. *Angew. Chem., Int. Ed.* **2006**, *45*, 1123–6.
(6) Dupont, J.; Suarez, P. A. Z.; De Souza, R. F.; Burrow, R. A.; Kintzinger, J.-P *Chem.—Eur. J.* **2000**, *6*, 2377–2381.
(7) Chiappe, C. In *Ionic Liquids in Synthesis*, 2d ed.; Wasserscheid, P. a. W. T., Ed.; Wiley -VCH: Weinheim, 2008; Vol. 1, pp 265−292.
(8) Bruzzone, S.; Malvaldi, M.; Chiappe, C. *Phys. Chem. Chem. Phys.* **2007**, *9*, 5576–5581.
(9) Chiappe, C. *Monatsh. Chem.* **2007**, *138*, 1035–1043.
(10) Padua, A. A. H.; Costa Gomes, M. F.; Canongia Lopes, J. N. A. *Acc. Chem. Res.* **2007**, *40*, 1087–1096.
(11) Hanke, C. G.; Johansson, A.; Harper, J. B.; Lynden-Bell, R. M. *Chem. Phys. Lett.* **2003**, *374*, 85–90.
(12) Holbrey, J. D.; Reichert, W. M.; Nieuwenhuyzen, M.; Sheppard, O.; Hardacre, C.; Rogers, R. D. *Chem. Commun.* **2003**, 476–477.
(13) Stepnowski, P.; Nichthauser, J.; Mrozik, W.; Buszewski, B. *Anal. Bioanal. Chem.* **2006**, *385*, 1483–1491.
(14) Zhang, J.; Huang, C.; Chen, B.; Ren, P.; Lei, Z. *Energy Fuels* **2007**, *21*, 1724–1730.
(15) Ma, J. C.; Dougherty, D. A. *Chem. Rev.* **1997**, *97*, 1303–1324.
(16) Reddy, A. S.; Sastry, G. N. *J. Phys. Chem. B* **2005**, *109*, 8893–8903.
(17) Yamada, S.; Saitoh, M.; Misono, T. *Tetrahedron Lett.* **2002**, *43*, 5853–5857.
(18) Inokuchi, F.; Miyahara, Y.; Inazu, T.; Shinkai, S. *Angew. Chem., Int. Ed.* **1995**, *34*, 1364–1366.
(19) Garel, L.; Lozach, B.; Dutasta, J.-P.; Collet, A. *J. Am. Chem. Soc.* **1993**, *115*, 11652–11653.
(20) Masci, B. *Tetrahedron* **1995**, *51*, 5459–5464.
(21) Holbrey, J. D.; Reichert, W. M.; Rogers, R. D. *Dalton Trans.* **2004**, 2267–2271.
(22) Koelle, P.; Dronskowski, R. *Inorg. Chem.* **2004**, *43*, 2803–2809.
(23) Hunt, P. A. *J. Phys. Chem. B* **2007**, *111*, 4844–4853.
(24) Welton, T. *Chem. Rev.* **1999**, *99*, 2071–2083.
(25) Welton, T. *Coord. Chem. Rev.* **2004**, *248*, 2459–2477.
(26) Magna, L.; Chauvin, Y.; Niccolai, G. P.; Basset, J.-M. *Organometallics* **2003**, *22*, 4418–4425.
(27) Billard, I.; Moutiers, G.; Labet, A.; El Azzi, A.; Gaillard, C.; Mariet, C.; Luetzenkirchen, K. *Inorg. Chem.* **2003**, *42*, 1726–1733.
(28) Canongia Lopes, J. N.; Deschamps, J.; Pádua, A. A. H. *J. Phys. Chem. B* **2004**, *108*, 2038–2047.
(29) Canongia Lopes, J. N.; Pádua, A. A. H. *J. Phys. Chem. B* **2004**, *108*, 16893–16898.
(30) Canongia Lopes, J. N.; Padua, A. A. H. *J. Phys. Chem. B* **2008**, *112*, 5039–5046.
(31) Jorgensen, W. L.; Maxwell, D. S.; Tirado-Rives, J. *J. Am. Chem. Soc.* **1996**, *118*, 11225–11236.
(32) Maginn, E. J. *Acc. Chem. Res.* **2007**, *40*, 1200–1207.
(33) Blanchard, L. A.; Brennecke, J. F. *Ind. Eng. Chem. Res.* **2001**, *40*, 287–292.
(34) Zhai, C.; Wang, J.; Zhao, Y.; Tang, J.; Wang, H. *Z. Phys. Chem.* **2006**, *220*, 775–785.
(35) Del Popolo, M. G.; Mullan, C. L.; Holbrey, J. D.; Hardacre, C.; Ballone, P. *J. Am. Chem. Soc.* **2008**, *130*, 7032–7041.
(36) Deetlefs, M.; Hardacre, C.; Nieuwenhuyzen, M.; Sheppard, O.; Soper, A. K. *J. Phys. Chem. B* **2005**, *109*, 1593–1598.
(37) Harper, J. B.; Lynden-Bell, R. M. *Mol. Phys.* **2004**, *102*, 85–94.
(38) Hanke, C. G.; Johansson, A.; Harper, J. B.; Lynden-Bell, R. M. *Chem. Phys. Lett.* **2003**, *374*, 85–90.
(39) Su, B.-M.; Zhang, S.; Zhang, Z. C. *J. Phys. Chem. B* **2004**, *108*, 19510–19517.
(40) Haigh, C. W.; Mallion, R. B. *Org. Magn. Reson.* **1972**, *4*, 203–28.
(41) Avent, A. G.; Chaloner, P. A.; Day, M. P.; Seddon, K. R.; Welton, T. *Dalton Trans.* **1994**, *3405*, 13.
(42) Frezzato, D.; Rastrelli, F.; Bagno, A. *J. Phys. Chem. B* **2006**, *110*, 5676–5689.
(43) Ämmälahti, E. B.; Molko, D.; Cadet, J. *J. Magn. Reson.* **1996**, *122*, 230–232.

(44) Clark, M.; Cramer, R. D., III; Van Opdenbosch, N. *J. Comput. Chem.* **1989**, *10*, 982–1012.

(45) Steward, J. J. P. *J. Comput. Chem.* **1991**, *10*, 320.

(46) Chipot, C.; Maigret, B.; Pearlman, D. A.; Kollman, P. A. *J. Am. Chem. Soc.* **1996**, *118*, 2998–3005.

(47) Canongia Lopes, J. N. A.; Padua, A. A. H. *J. Phys. Chem. B* **2006**, *110*, 3330–3335.

(48) Canongia Lopes, J. N.; Costa Gomes, M. F.; Padua, A. A. H. *J. Phys. Chem. B* **2006**, *110*, 16816–16818.

(49) Lachwa, J.; Bento, I.; Duarte, M. T.; Lopes, J. N. C.; Rebelo, L. P. N. *Chem. Commun.* **2006**, 2445–2447.

(50) Hunt, P. A.; Kirchner, B.; Welton, T. *Chem.—Eur. J.* **2006**, *12*, 6762–6775.

(51) Yoshida, Y.; Baba, O.; Larriba, C.; Saito, G. *J. Phys. Chem. B* **2007**, *111*, 12204–12210.

(52) Katsyuba, S. A.; Dyson, P. J.; Vandyukova, E. E.; Chernova, A. V.; Vidis, A. *Helv. Chim. Acta* **2004**, *87*, 2556–2565.

(53) Kobrak, M. N. *J. Phys. Chem. B* **2007**, *111*, 4755–4762.

(54) Cutting, B.; Ghose, R.; Bodenhausen, G. *J. Magn. Reson.* **1999**, *138*, 326–329.

(55) Smith, W.; Forester, T. R.; Todorov, I. T. *The DL_POLY molecular simulation package*, 2.18 ed.; T. D. P. m. s., Ed.; STFC Daresbury Laboratorys: Warrington, UK, 2007.

JP805573T